Dalton Transactions

ROYAL SOCIETY OF CHEMISTRY

PAPER

View Article Online
View Journal | View Issue

Check for updates

Cite this: *Dalton Trans.*, 2024, **53**, 11858

Preparation of seven-coordinated hypervalent tin(IV)-fused azobenzene and applications for stimuli-responsive π-conjugated polymer films†

Masayuki Gon, [a,b] Yusuke Morisaki,[a] Kazuya Tanimura[a] and Kazuo Tanaka *[a,b]

Received 14th June 2024,
Accepted 27th June 2024

DOI: 10.1039/d4dt01738b

rsc.li/dalton

Heavy atoms can form highly coordinated states, and their optical properties have attracted much attention. Recently, we have demonstrated that a reversible coordination-number shift of hypervalent tin(IV) from five to six can provide predictable hypsochromic shifts in light absorption and emission properties in small molecules and a π-conjugated polymer film. Herein, we show the preparation of seven-coordinated tin and reveal that the binding constant of the seven coordination with ethylenediamine (EDA, K = 2900 M^{-1}) is 200 times higher than that of six coordination with propylamine (PA, K = 14 M^{-1}) owing to the chelate effect. Moreover, reversible vapochromism of the π-conjugated polymer film was observed upon exposure (λ_{abs} = 598 nm and λ_{PL} = 697 nm) and desorption (λ_{abs} = 641 nm and λ_{PL} = 702 nm) of EDA vapor. Furthermore, as a unique demonstration, the thermochromic film was prepared by fixing the seven coordination as the initial state using 1,10-phenanthroline. These optical variations are predictable by quantum chemical calculations. Our findings are valuable for the development of designable and controllable stimuli-responsive materials focusing on the inherent properties of the elements.

Introduction

Owing to the large atomic size and wide coordination space, heavy atoms are capable of forming more highly-coordinated states than four-coordinated states, and the structural properties of the resulting compounds have attracted much attention.[1–3] Their coordination flexibility allows the coordination-number shift caused by environmental changes and therefore has been applied as a key component for developing chemical reactions[4–7] and stimuli-responsive systems.[8,9] In the main group elements, the highly-coordinated states can be classified as hypervalent states beyond the octet rule, where hypervalent compounds are characterized by the formation of relatively polarized three-center four-electron (3c–4e) bonds without d orbitals.[10–14]

Tin (Sn) is one of the heavy group 14 elements, and it is known that the hypervalent tin(IV) compounds have various coordination numbers, five,[15–22] six,[23–29] seven,[30–35] and eight.[36] Therefore, their structural features and physical properties have been explored. For example, based on the coordination-state shift, followed by optical changes, which can be dynamically controlled by temperature[37] and addition of ligands,[38] turn-off luminescent chemosensors have been developed.[38] On the other hand, there are still much room for exploring the difference of electronic properties, such as light absorption and luminescence characters, depending on the coordination numbers and for applying their environmental sensitiveness as a stimuli-responsive material. In addition, most research on hypervalent compounds has focused on the fundamental properties of isolated molecules and has rarely been applied to polymer materials. If hypervalent compounds are composited into polymer matrices, they are isolated from the external environment, which makes it difficult to exploit their stimuli-responsive abilities. Therefore, it is essential to develop a novel method for developing polymer materials based on hypervalent compounds.

π-Conjugated polymers have excellent optoelectronic properties derived from their delocalized π-electrons through rigid backbones.[39] Owing to these unique properties, conjugated polymers have been widely applied as a key component in organic devices and materials, such as organic light-emitting diodes (OLEDs),[40] organic photovoltaics (OPVs),[41] and bioimaging probes.[42] Among them, the π-conjugated polymers which change their optical properties in response to external

[a]*Department of Polymer Chemistry, Graduate School of Engineering, Kyoto University Katsura, Nishikyo-ku, Kyoto 615-8510, Japan. E-mail: tanaka@poly.synchem.kyoto-u.ac.jp*
[b]*Graduate School of Global Environmental Studies, Kyoto University, Katsura, Nishikyo-ku, Kyoto 615-8510, Japan*

†Electronic supplementary information (ESI) available. CCDC 2349665 and 2349666. For ESI and crystallographic data in CIF or other electronic format see DOI: https://doi.org/10.1039/d4dt01738b

stimuli are expected to work as sensing materials.[43–45] These stimulus-responsive π-conjugated systems enable simple and speedy assessments for surrounding environment and health condition without complicated and expensive devices. Environmental sensitivity has been often induced by introducing heteroatom into the polymer chains of conjugated polymers, and the resulting stimuli-responsive polymers have been applied as a scaffold for chemoselective detectors.[46–50] In particular, a very few examples of film-type chemical sensors were fabricated despite of their high applicability,[51] and therefore there are great demand for development of polymer materials using novel stimuli-responsive systems taking advantage of elements.

We recently proposed various types of stimuli-responsive π-conjugated polymer materials.[52–60] We also focused on the unique optical properties based on hypervalency of heavy atoms, and reported germanium, tin, and bismuth-fused azobenzene compounds (GAz,[61,62] TAz,[63–65] and BiAz,[66] respectively). In particular, it was found that the variable coordination-numbers of TAz from five to six by coordination of nucleophiles such as dimethyl sulfoxide (DMSO) induced the hypsochromic shift of absorption and emission bands.[63] According to the mechanistic studies, it was found that the coordination should cause electronic perturbation at the directly-linked π-conjugated system through the 3c–4e bond and the tin–nitrogen (Sn–N) bond. These changes in optical properties were also observed in film consisting of the π-conjugated polymer containing TAz as a repeating unit, and it was confirmed that TAz compounds play a key role in stimuli-responsiveness.[65]

Herein, we show synthesis and electronic properties of the higher coordination state, seven coordination, of TAz derivatives from small molecules to polymers and applications as optical sensors to demonstrate wide versatility. We confirmed the formation of the seven-coordinated TAz in both solid and solution with ethylenediamine (EDA) as a bidentate ligand and observed the changes in the optical properties by the coordination-number shift from five to seven. The chelate effect of EDA having stronger interactions than DMSO and propylamine (PA) was revealed. The π-conjugated polymer films containing TAz moieties showed vapochromism upon exposure to the EDA vapor, and the correlation of chromism with the coordinating ability of vapor molecules was clarified. Moreover, as a unique application of our findings, we constructed the thermochromic film by employing coordination and heat-triggering irreversible release of 1,10-phenanthroline (phen) in film. We accomplished to fix the seven-coordination state in film and set it as the initial state. Optical changes were then observed by heating through releasing the ligand. It should be emphasized that these coordination processes were predictable by strength of coordination estimated by quantum calculations. From the series of experiments and discussions described here, not only fundamental properties and regulation of the seven-coordination state of hypervalent tin but also wide applicability for logical design of sensors according to quantum calculations are demonstrated.

Results and discussion

Synthesis

Scheme 1 shows the synthesis of the TAz compounds. **TAz** and **P-TAz** were prepared according to the literature.[65] The polymerization was carried out by the Migita–Kosugi–Stille cross-coupling reaction[67,68] with **TAz** and (9,9-di(2,5,8,11-tetraoxatridecan-13-yl)-9*H*-fluorene-2,7-diyl)bis(trimethylstannane) (**1**) in the catalytic system of $Pd_2(dba)_3$ (dba = dibenzylideneacetone) and XPhos (2-dicyclohexylphosphino-2′,4′,6′-triisopropylbiphenyl) to obtain **P-TAz** (M_n = 18 800, M_w/M_n = 4.3). The newly prepared **P-TAz** had the higher molecular weight than that obtained in our previous research.[65] The tetraethylene glycol side chains were introduced to improve solubility and affinity to solvent molecules regardless of polarity. The number and weight average molecular weights (M_n and M_w) were determined by a gel permeation chromatography (GPC) using chloroform ($CHCl_3$) as an eluent with polystyrene standards. **P-TAz** was characterized by ^1H, $^{13}C\{^1H\}$ and ^{119}Sn NMR spectroscopy and matrix-assisted laser desorption/ionization-time of flight mass spectrometry (MALDI-TOF MS) in ESI.† These characterization data allow us to investigate the properties of the obtained compounds.

Amine coordination

The coordination of amine derivatives to **TAz** in solution was investigated by ^1H and ^{119}Sn NMR spectroscopy. To evaluate the coordination numbers of **TAz** in the presence of amine derivatives, ^{119}Sn NMR measurements of **TAz** in benzene-d_6, propylamine (PA), and ethylenediamine (EDA) were performed (Fig. 1a). For comparison, the same measurement was executed in dimethyl sulfoxide (DMSO). In this case, it is strongly suggested that TAz derivatives should form the six-coordinated structures that are able to be identified by ^{119}Sn NMR spectroscopy.[65] Consequently, we found that the ^{119}Sn NMR signal in PA and DMSO showed the large upfield shifts from that in benzene-d_6. These results suggest that PA and DMSO, which are monodentate ligands, should coordinate to tin, and **TAz** formed six-coordinated structures in these solutions. Significantly, in EDA, which can work as a bidentate ligand, the further upfield shift was observed. This fact strongly indi-

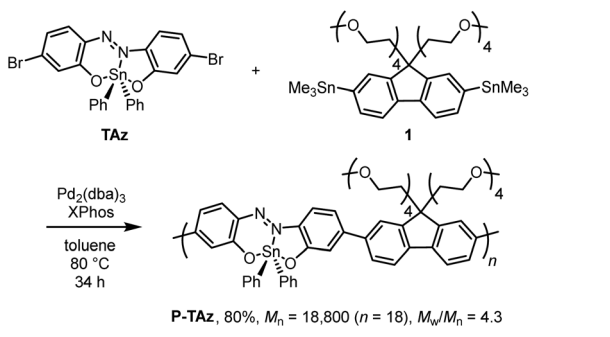

Scheme 1 Synthesis of **P-TAz**. The regiorandom polymer was obtained, and this certain structure is shown here.

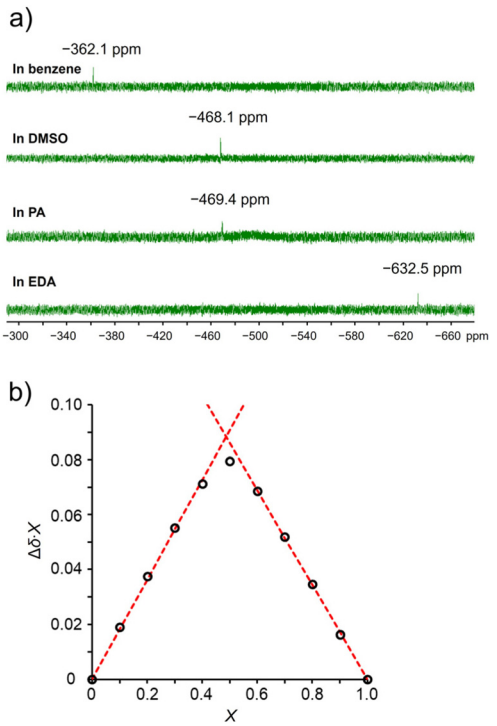

Fig. 1 (a) ^{119}Sn NMR spectra of **TAz** in benzene, DMSO, PA and EDA. (b) The ^{1}H NMR Job plot for the binding of **TAz** with EDA (total concentration = 10 mM) in benzene-d_6.

cates the formation of the seven-coordinated structure of **TAz** because the ^{119}Sn NMR chemical shifts in the seven-coordinate compounds are known to be more than 100 ppm upfield from those in the six-coordinate analogues.[69] To further evaluate the binding mode, we made a job plot of the ^{1}H NMR in benzen-d_6 (Fig. 1b). In the Job plot,[70] a horizontal and a vertical axis represents the mole fraction (X) and the product of the change in the NMR peak and the mole fraction ($\Delta\delta{\cdot}X$), respectively. The value of X, which represents the maximum value of $\Delta\delta{\cdot}X$, indicates the host and guest equivalents. Accordingly, the value of X was maximum at 0.49, suggesting 1 : 1 complexes of **TAz** and EDA.

Crystal structure

We attempted to prepare a co-crystal of **TAz** and EDA to obtain structural information of the seven-coordinated **TAz**. Fortunately, the crystal was sufficiently grown in $CHCl_3$ by a vapor diffusion method in the presence of EDA. We also prepared a single crystal of **TAz** to evaluate the structural differences between the five and seven coordination. Fig. 2 illustrates the structures of **TAz** and its EDA adduct (**TAz-EDA**) determined by a single crystal X-ray diffraction (SC-XRD) analysis. Detailed crystallographic data are shown in Tables S1–S3 and Fig. S1, S2.† **TAz** showed the five-coordinated tin and distorted trigonal bipyramidal geometry with two oxygens (O(1) and O(2)) at apical positions and one nitrogen (N(1)) and two carbons in the phenyl groups at equatorial positions. Corresponded to the data from the Job plot, it was shown that

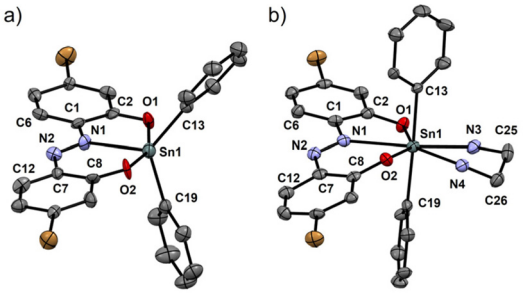

Fig. 2 ORTEP drawings of (a) **TAz** and (b) **TAz-EDA**. Thermal ellipsoids are scaled to the 50% probability level. Hydrogen and disordered atoms are omitted to clarify. All crystallographic data are shown in ESI.† CCDC 2349665 for **TAz** and 2349666 for **TAz-EDA**.†

TAz-EDA has the seven-coordinated tin in which two nitrogen atoms of EDA are bound to the tin center to form a pentagonal bipyramidal geometry. In this structure, two carbons of phenyl groups occupy apical positions with the C(13)–Sn(1)–C(19) bond angle of 178.0°, and other atoms are arranged in the equatorial plane. The structural features are similar to the other seven-coordinated tin compounds with the bidentate ligands.[33–35] In the five-coordinated structure of **TAz**, the small C(6)–C(1)–N(1)–N(2) and N(1)–N(2)–C(7)–C(8) dihedral angles at 4° and 8° show high planarity of the azobenzene skeleton, respectively. Although these dihedral angles increase in the seven-coordinated structure (8.3° for C(6)–C(1)–N(1)–N(2) and 12.6° for N(1)–N(2)–C(7)–C(8)), the planarity of azobenzene backbone can be considerably maintained. This result indicates that the optical properties, which are highly dependent on the planarity of the π-plane, should be retained in the seven-coordinated structure. In addition, the coordination of EDA induces bond elongation of Sn(1)–O(1), Sn(1)–O(2), and Sn(1)–N(1) (+0.10 Å, +0.15 Å, and +0.22 Å, respectively) from the five-coordinated **TAz**. This suggests that the dramatic change in the electronic states of **TAz** should be caused by the coordination of EDA.

Optical properties

First, UV–vis absorption spectra were measured to investigate the effects of the coordination at the tin atom with amine derivatives on electronic properties of **TAz** in the ground state (Fig. 3a, c and Table 1). Hypsochromic shifts of the absorption band were observed by adding PA or EDA in toluene. We also performed UV–vis spectrophotometric titrations with both amines (Fig. S3†). As a result, even in the presence of small amount of EDA, the drastic bathochromic shift was detected, suggesting that **TAz** can form stronger interaction with EDA than PA. In both titration experiments, the isosbestic points were observed in the spectra when the small amount of amines was added, implying that the coordination could proceed with a 1 : 1 binding ratio.[63,65] These data correspond to those from the Job plot and SC-XRD. Next, to examine the electronic properties in the excited states, we measured the photoluminescence (PL) spectra of **TAz** with or without PA and

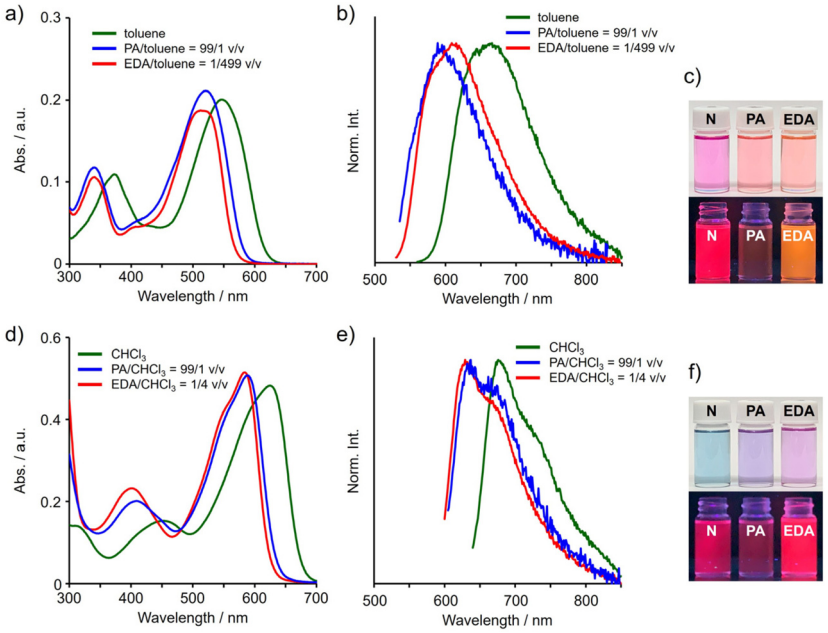

Fig. 3 (a) UV–vis absorption, (b) PL spectra, and (c) photographs of **TAz** in the mixed solvent of toluene and amines (1.0×10^{-5} M), excited at λ_{abs} for PL, under room right (upper) and irradiation by UV lamp (365 nm) (lower) for photographs. The spectral changes were saturated in PA/toluene = 99/1 v/v and EDA/toluene = 1/499 v/v. (d) UV–vis absorption, (e) PL spectra, and (f) photographs of **P-TAz** in mixed solvent of $CHCl_3$ and amines (1.0×10^{-5} M per repeating unit), excited at λ_{abs} for PL, under room right (upper) and irradiation by UV lamp (365 nm) (lower) for photographs. The spectral changes were saturated in PA/$CHCl_3$ = 99/1 v/v and EDA/$CHCl_3$ = 1/4 v/v. N in the photographs means no amine.

Table 1 Spectroscopic data of **TAz** and **P-TAz** in mixed solution[a]

	Solvent	λ_{abs}/nm	λ_{PL} [e]/nm	Φ_{PL} [e,f]/%
TAz	Toluene	547	666	15.6
	PA[b]	521	589	1.0
	EDA[c]	513	609	5.5
P-TAz	$CHCl_3$	625	676	23.5
	PA[b]	589	637	1.0
	EDA[d]	584	629	7.4

[a] 1.0×10^{-5} M for **TAz**, 1.0×10^{-5} M per repeating unit for **P-TAz**. [b] PA/toluene = 99/1 v/v (PA: 1.2×10^{6} eq.). [c] EDA/toluene = 1/499 v/v (EDA: 3×10^{3} eq.). [d] EDA/$CHCl_3$ = 1/4 v/v (EDA: 3×10^{5} eq.). [e] Excited at λ_{abs}. [f] Absolute PL quantum yield.

EDA (Fig. 3b, c and Table 1). The emission of **TAz** was gradually quenched as the amount of amines increased, accompanied by hypsochromic shifts of the emission bands in the PL spectra (Fig. S3†). These results mean that the coordination of PA and EDA can be maintained not only in the ground state but also in the excited state.[71]

To investigate the coordination behavior of amine derivatives to the TAz moieties in the π-conjugated polymer, the titration experiment with **P-TAz** in $CHCl_3$ was performed (Fig. 3d, f, S4† and Table 1). $CHCl_3$ was used as a good solvent for **P-TAz** instead of the poor solvent, toluene. Basically, the polymer showed a similar trend in optical properties to **TAz**, while the larger amount of amines was needed to reach a plateau in the spectral changes. It is probably due to the higher polarity of $CHCl_3$ than that of toluene. This suggests that the coordination of PA and EDA can occur at the TAz moieties in the π-conjugated polymer main chains. In addition, the absolute PL quantum yield (Φ_{PL}) was higher in **P-TAz** than that in **TAz**. This increase in emission efficiency could be attributed to the increase in the overlap of π and π* orbitals and the enhancement of rigidity of the polymer backbone because of the extension of the π-conjugated systems. Modulation of optical properties by changing the coordination states was also shown in the π-conjugated polymer.

Binding constants

To quantify the interaction between the amine derivatives and **TAz**, we estimated a binding constant (K) using a curve fitting method with the spectra from the UV–vis spectrophotometric titration in toluene under the assumption of 1 : 1 coordination (Fig. S5†).[63,65] The estimated K and chemical structures of the amine derivatives are shown in Fig. 4. The bidentate ligand EDA showed 200 times the higher K value than the monodentate ligand PA. This is attributed to strong stabilization of the 1 : 1 complex owing to the chelate effect. The K value of PA was similar to that of the previously reported monodentate ligand, DMSO.[65] The smaller K values were observed from *N*,*N*,*N*′,*N*′-tetramethylethylenediamine (TMEDA) and *N*,*N*′-dimethylethylenediamine (DMEDA) than that of EDA. It is likely that the coordination should be disturbed due to the steric hindrance. In addition, the bidentate ligand 1,3-propanediamine (PDA) showed smaller K than EDA. This fact indicates that the formation of a five-membered ring is preferable to that of a six-membered ring. The largest K value was obtained from

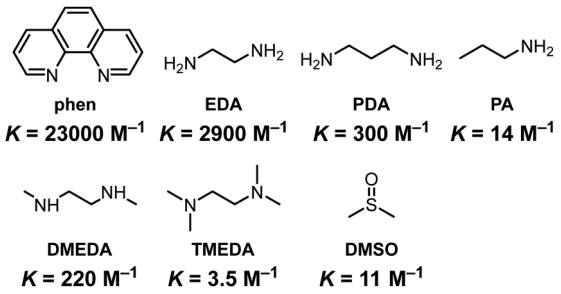

Fig. 4 Molecular structures and binding constants (K) to **TAz** of N-ligands in toluene. The K value of DMSO was previously reported (ref. 65).

phen. It is because of the rigid structure in addition to the formation of the five-membered ring. In $CHCl_3$, K was 10 times lower than in toluene probably due to its higher polarity (Fig. S6†). This is one of the reasons why the larger amounts of PA and EDA are needed to saturate the spectral changes in the UV–vis absorption and PL of **P-TAz**.

Theoretical calculations

To gather deeper insight on electronic properties, we performed quantum chemical calculations with density functional theory (DFT) and time-dependent (TD)-DFT. The detailed protocols are shown in ESI.† Since the crystal structure of the adduct of **TAz** and PA (**TAz-PA**) was not able to be determined from the SC-XRD analysis, the structure was optimized by replacing DMSO to PA based on the DMSO adduct reported in our previous literature.[65] Consequently, the optimized structures in the ground state showed high planarity of the azobenzene skeletons in the five-, six-, and seven-coordinated structures (Fig. 5). The distributions of the highest occupied molecular orbitals (HOMOs) and the lowest unoccupied molecular orbitals (LUMOs) of the six and seven-coordinated structures were similar to those of the five-coordinated structure, and the amine coordination to the tin hardly disturbed the π-system (Fig. 6 and S7†). On the other hand, both of the HOMO and LUMO energy levels were elevated by the amine coordination, especially in the seven coordination. In particular, the increases in the LUMO energy levels of both the six- and seven-coordinated structures were larger than those in the HOMO energy levels, and their energy gaps were almost equal but larger than that of the five-coordinated structure. These results were in good qualitative agreement with experimental data where the addition of PA and EDA caused similar hypsochromic shifts of the optical bands in the UV–vis absorption spectra (Table S4†). The bond lengths of Sn(1)–N(1) in the optimized structures were longer in the order of five coordination (2.25 Å for **TAz**), six coordination (2.32 Å for **TAz-PA**), and seven coordination (2.37 Å for **TAz-EDA**), which qualitatively correlate with the binding constants.

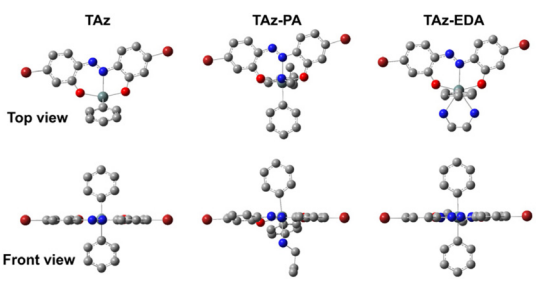

Fig. 5 Optimized structures of **TAz**, **TAz-PA** and **TAz-EDA** obtained with DFT calculations.

We also performed a natural bond orbital (NBO) calculation to evaluate the contribution of the molecular orbitals in detail.[72,73] As a consequent, it was proposed that the coordination of PA and EDA raises the HOMO and LUMO energy levels *via* oxygens and nitrogen by increasing the electron density around tin. The donor–acceptor interaction between LP(N1) and LP*(Sn1) was weakened by the coordination of PA and EDA, indicating the decrease in the electron-accepting ability of tin followed by the increase in the energy levels of the directly-linked azo moiety (Fig. S8†). In addition, the energy levels of LP(O1) and LP(O2) of **TAz-EDA** were elevated compared to **TAz**, meanwhile slight changes were observed in **TAz-PA** (Fig. S9†). These results suggest that more excess electrons at the seven-coordinated tin should be delocalized *via* oxygens through azobenzene skeletons. Consequently, the elevations of the energy levels of frontier molecular orbitals are induced. Furthermore, the origin of optical properties of TAz moieties during the coordination-number shift from five to six or seven should be not distorting the π-conjugated systems but larger degree of increase in the HOMO energy level through oxygens and nitrogen.

We also conducted similar calculations with **M-TAz** as a model compound for the polymer (Fig. 6 and Table S4†). The HOMO and LUMO of **M-TAz** extended through the fluorene moieties and their energy levels were altered, similarly to those of **TAz** by the amine coordination. These results propose that the TAz moieties should be responsible for electronic property changes of main-chain conjugation. In other words, TAz moieties are able to play a critical role in electronic property changes of π-conjugated polymers as a switching module.

Development of film-type vapochromic materials

We directly applied the chromism by the coordination-number shift for constructing film-type vapochromic materials. The thin film of **P-TAz** was prepared with a spin-coating method (1000 rpm, 30 s) on the quartz substrate (2.5 cm × 0.9 cm) from the $CHCl_3$ solution (50 μL of (1 mg per 300 μL)). Exposure of the film to EDA vapor caused hypsochromic shifts in both the absorption and emission bands in the spectra (Fig. 7, S10, and Table S5†). Furthermore, by heating at 80 °C after the exposure, the shapes of the spectra were restored to the initial states. These data indicate that the coordination-number shift followed by optical property changes proceed reversibly. Additionally, we confirmed that these spectrum changes were able to be repeated at least 5 times. The strength of the interaction between **TAz** and vapor molecules is domi-

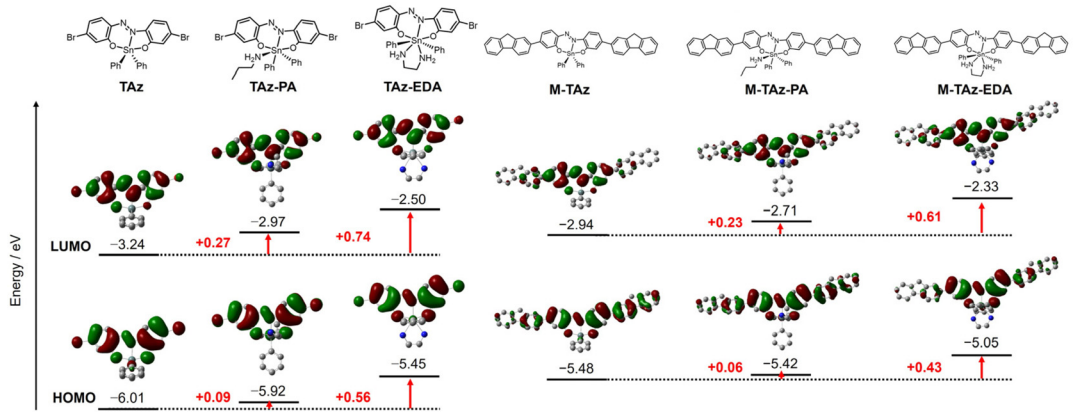

Fig. 6 Energy diagrams and selected MOs of **TAz**, **TAz-PA**, **TAz-EDA**, **M-TAz**, **M-TAz-PA**, and **M-TAz-EDA** obtained with DFT calculations (isovalue = 0.02). Hydrogen atoms are omitted for clarity.

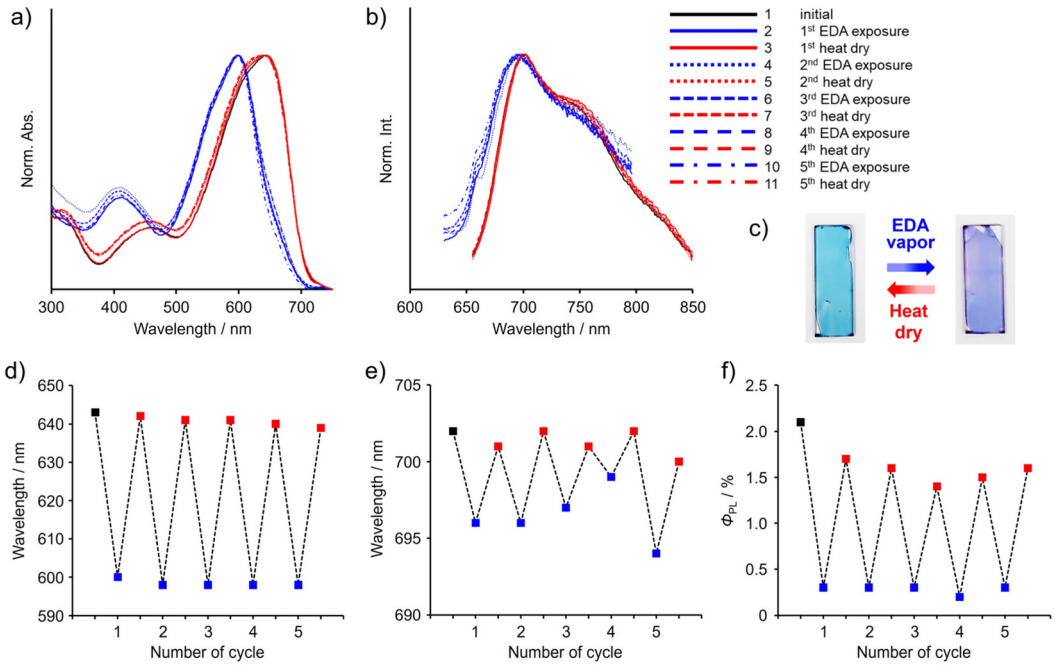

Fig. 7 Reversible controls of (a and d) UV–vis absorption, (b and e) PL properties, (c) photographs under room right, and (f) absolute PL quantum yields of **P-TAz** in film upon exposure to EDA vapor and dry processes (80 °C for 3 min on the hot plate). The detailed method and spectroscopic data are shown in Fig. S9 and Table S5,† respectively.

nant in our system, and in fact, DMSO, PA and EDA were able to be captured. In contrast, sensitivity in vapor-responsive behaviors based on the coordination, as seen in conventional complexes, strongly depends on volatility of vapor molecules which is represented as vapor pressure.[74–77] In fact, the recovery time and conditions of the films after exposure to vapors significantly depended on the type of vapors. The films exposed to DMSO and PA were almost recovered by vacuum drying at room temperature for three minutes, meanwhile the appearance of the film exposed to EDA vapor was hardly altered by the same treatment (Fig. S11†). The short recovery time of the film exposed to PA may be due to the high volatility of PA (vapor pressure = 33.9 kPa at 20 °C). On the other hand, considering that EDA (vapor pressure = 1.4 kPa at 20 °C) has much higher vapor pressure than DMSO (vapor pressure = 59.4 Pa at 20 °C), insensitivity of the EDA-coordinated film toward heating could be originated from stronger interaction between **TAz** and EDA than DMSO. It should be mentioned that we introduced the tetraethylene glycol side chains, which have amphiphilicity, into the comonomer units.[65] Therefore, it was expected that penetration of solvent vapor molecules even with high polarity through the polymer film could be enhanced owing to high miscibility. Hence, it might be potentially suitable for constructing vapor sensors because a wide

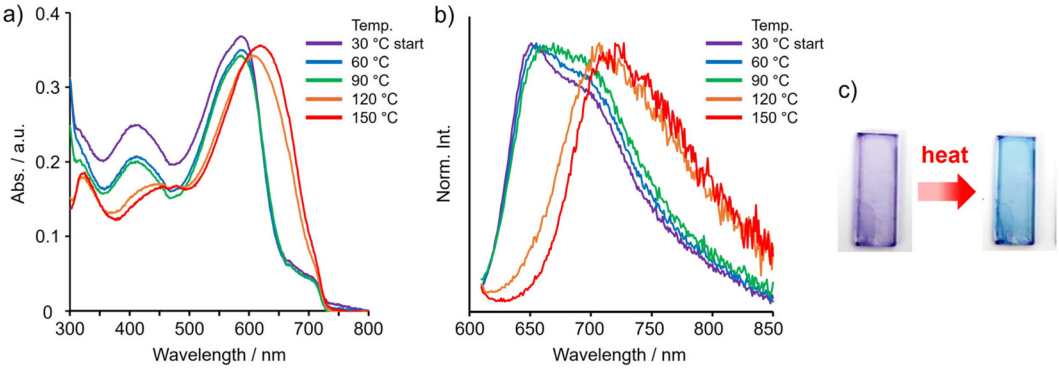

Fig. 8 (a) Changes in UV–vis absorption and (b) PL spectra by heating and (c) photographs of theremochromic behaviors of the film containing **P-TAz** and phen under room light.

variety of coordinating solvents could be applicable. In summary, from these results, it is clearly demonstrated that the coordination-number shift of **TAz** can be a key mechanism for developing optical film sensors. Moreover, it is proposed that it might become possible to detect even low vapor pressure gasses that are difficult to measure with conventional sensors based on the coordination-number shift of hypervalent tin.

Application for film-type thermochromic materials

We finally demonstrate unique application to construct a thermometer based on the chromism by molecular coordination at hypervalent tin. It was difficult to fix the seven-coordinated state of tin in the polymer film with solvent vapors due to their spontaneous desorption. By using the solid ligand phen instead of volatile amines, we presumed to obtain stable films containing seven-coordinated tin and subsequently to be capable of releasing phen by heating. Based on this heat-triggered coordination-number shift from seven to five with chromism, we expected to obtain thermochromic materials. The films were prepared by the spin-coating method (1000 rpm, 30 s) on the quartz substrate (2.5 cm × 0.9 cm) from a mixed $CHCl_3$ solution of phen and **TAz-Ph** (50 μL of **P-TAz** (1 mg) and phen (5 mg) per 300 μL). The initial color of the resulting film was purple, suggesting that the seven-coordinated TAz moieties should be obtained. It was found that both absorption and emission bands in the spectra were bathochromically shifted by heating around 90–120 °C (Fig. 8 and Table S6†), and, as we expected, clear thermochromic behaviors from purple to greenish-blue were observed. This should be because of the thermal desorption of phen in the film accompanied by the coordination-number shift of tin from seven to five. It should be mentioned that the spectra did not return even after cooling. After color change, we dissolved the film in $CHCl_3$ and subsequently dried the solution. Consequently, the purple residue was obtained (Fig. S12†). It is because desorption of phen followed by diffusion through polymer matrices should occur. Interestingly, from the thermogravimetric analysis (TGA) and differential scanning calorimetry (DSC) measurements, it was revealed that evaporation of phen in the **P-TAz** film should also proceed without any degradation of the tin compounds (Fig. S13†). Since evaporation of phen was hardly detected when the crystalline sample of phen was heated, evaporation might be observable only in the polymer matrices where each molecule should be isolated. This evaporation process would also contribute to suppressing re-coordination of phen with the tin atom. The width of the band shift caused by the phen desorption was larger than that by EDA especially in PL spectra. Considering the facts that larger spectroscopic changes were induced by phen than by EDA, and the phen-coordinating compounds had the similar extents of estimated transition energies as the TAz and EDA ones (Table S4†), we assume that the stronger interaction could be formed between **P-TAz** and phen than EDA. These stronger interaction could cause larger degree peak shifts in the optical spectra. In summary, we were able to immobilize a seven-coordinated state by selecting an appropriate ligand. Furthermore, the ligand desorption was able to be induced by heating. Finally, based on these coordination properties, thermochromic film materials with tunable properties were demonstrated. From this result, versatility of our system can be revealed.

Conclusion

In this study, we reveal the reversible coordination-number shift from five to seven followed by the alteration of their optical properties in the hypervalent tin(IV)-fused azobenzene compounds. The bidentate amine ligands can strongly coordinate to tin through the chelate effect and subsequently change the optical properties of the TAz derivatives. According to theoretical calculations, it was suggested that the hypsochromic shift should be originated from the asymmetric elevation of the energy levels of LUMO over HOMO triggered by the formation of the seven-coordinated structure followed by the increase in the electron density at the tin atom. It was also demonstrated that optical properties of π-conjugated polymers are able to be regulated by changing the coordination number at the TAz unit. Moreover, based on the coordination-number

shift, we accomplished the observation of vapochromic behaviors with thin films of **P-TAz** upon exposure to amine vapors. EDA vapor induced clear color changes of the films by the coordination. According to theoretical investigation, correlation between the coordinating ability of the vapor and vapochromic behaviors was obtained. Furthermore, regarding the seven-coordinated state created by coordinating phen to **P-TAz** as the initial state, thermochromic behavior was achieved through the release of the ligand by heating and the subsequent color change. These results represent the applicability of the reversible coordination-number shift from five to seven followed by the alteration of their optical properties in the hypervalent tin(IV) compounds as a platform not only for stimuli-responsive π-conjugated systems but also for designable chromic materials.

Data availability

All experimental and characterization data and detailed experimental procedures are available in the published article and ESI.†

Conflicts of interest

There are no conflicts to declare.

Acknowledgements

This work was partially supported by the Izumi Science and Technology Foundation (for M. G.), a Grant-in-Aid for Scientific Research (B) (for M. G.) (JP23K23398) and (for K. T.) (JP24K01570).

References

1 K. Akiba, *Heteroat. Chem.*, 2011, **22**, 207–274.
2 C. I. Raț, C. Silvestru and H. J. Breunig, *Coord. Chem. Rev.*, 2013, **257**, 818–879.
3 R. Kumar, T. Dohi and V. V. Zhdankin, *Chem. Soc. Rev.*, 2024, **53**, 4786–4827.
4 J. Hyvl, *Dalton Trans.*, 2023, **52**, 12597–12603.
5 A. Yoshimura, A. Saito and V. V. Zhdankin, *Adv. Synth. Catal.*, 2023, **365**, 2653–2675.
6 M. Benaglia, S. Guizzetti and L. Pignataro, *Coord. Chem. Rev.*, 2008, **252**, 492–512.
7 N. Asok, J. R. Gaffen and T. Baumgartner, *Acc. Chem. Res.*, 2023, **56**, 536–547.
8 N. Kano, M. Yamamura and T. Kawashima, *Dalton Trans.*, 2015, **44**, 16256–16265.
9 J. R. Gaffen, J. N. Bentley, L. C. Torres, C. Chu, T. Baumgartner and C. B. Caputo, *Chem*, 2019, **5**, 1567–1583.
10 J. I. Musher, *Angew. Chem., Int. Ed. Engl.*, 1969, **8**, 54–68.
11 A. E. Reed and F. Weinhold, *J. Am. Chem. Soc.*, 1986, **108**, 3586–3593.
12 G. C. Pimentel, *J. Chem. Phys.*, 1951, **19**, 446–448.
13 R. J. Hach and R. E. Rundle, *J. Am. Chem. Soc.*, 1951, **73**, 4321–4324.
14 T. Atsumi, T. Abe, K. Akiba and H. Nakai, *Bull. Chem. Soc. Jpn.*, 2010, **83**, 892–899.
15 G. Sahu, S. A. Patra, P. D. Pattanayak and R. Dinda, *Chem. Commun.*, 2023, **59**, 10188–10204.
16 K. E. Bessler, J. A. dos Santos, V. M. Deflon, S. de Souza Lemos and E. Niquet, *Z. Anorg. Allg. Chem.*, 2004, **630**, 742–745.
17 H. Reyes, C. García, N. Farfán, R. Santillan, P. Lacroix, C. Lepetit and K. Nakatani, *J. Organomet. Chem.*, 2004, **689**, 2303–2310.
18 S. M. Crawford, A. Al-Sheikh Ali, T. S. Cameron and A. Thompson, *Inorg. Chem.*, 2011, **50**, 8207–8213.
19 M. Yamamura, M. Albrecht, M. Albrecht, Y. Nishimura, T. Arai and T. Nabeshima, *Inorg. Chem.*, 2014, **53**, 1355–1360.
20 M. Saito, S. Imaizumi, T. Tajima, K. Ishimura and S. Nagase, *J. Am. Chem. Soc.*, 2007, **129**, 10974–10975.
21 S. Tsukada, N. J. O'Brien, N. Kano, T. Kawashima, J.-D. Guo and S. Nagase, *Dalton Trans.*, 2016, **45**, 19374–19379.
22 B. Glowacki, M. Lutter, D. Schollmeyer, W. Hiller and K. Jurkschat, *Inorg. Chem.*, 2016, **55**, 10218–10228.
23 E. Jakubikova, I. H. Campbell and R. L. Martin, *J. Phys. Chem. A*, 2011, **115**, 9265–9272.
24 A. S. Gowda, T. S. Lee, M. C. Rosko, J. L. Petersen, F. N. Castellano and C. Milsmann, *Inorg. Chem.*, 2022, **61**, 7338–7348.
25 V. G. K. Das, L. K. Mun, C. Wei and T. C. W. Mak, *Organometallics*, 1987, **6**, 10–14.
26 N. Chiorean, C. Coza, A. Pop and A. Silvestru, *J. Organomet. Chem.*, 2019, **880**, 83–90.
27 E. López-Torres, A. L. Medina-Castillo, J. F. Fernández-Sánchez and M. A. Mendiola, *J. Organomet. Chem.*, 2010, **695**, 2305–2310.
28 E. Guzmán-Percástegui, J. G. Alvarado-Rodríguez, J. Cruz-Borbolla, N. Andrade-López, R. A. Vázquez-García, R. N. Nava-Galindo and T. Pandiyan, *Cryst. Growth Des.*, 2014, **14**, 3742–3757.
29 J.-K. Park, W.-S. Kim, G. Otgondemberel, B.-J. Lee, D.-E. Kim and Y.-S. Kwon, *Colloids Surf., A*, 2008, **321**, 266–270.
30 D. Dakternieks, H. Zhu, D. Masi and C. Mealli, *Inorg. Chim. Acta*, 1993, **211**, 155–160.
31 G. F. de Sousa, J. Valdes-Martínez, G. E. Perez, R. A. Toscano, A. Abras and C. A. L. Filgueiras, *J. Braz. Chem. Soc.*, 2002, **13**, 559–564.
32 M. Gielen, M. Acheddad, M. Bouâlam, M. Biesemans and R. Willem, *Bull. Soc. Chim. Belg.*, 1991, **100**, 743–746.
33 T. S. Basu Baul, C. Masharing, R. Willem, M. Biesemans, M. Holčapek, R. Jirásko and A. Linden, *J. Organomet. Chem.*, 2005, **690**, 3080–3094.
34 A. Ramírez-Jiménez, E. Gómez and S. Hernández, *J. Organomet. Chem.*, 2009, **694**, 2965–2975.

35 I. V. Krylova, L. D. Labutskaya, M. O. Markova, V. A. Balycheva, P. G. Shangin, A. Y. Akyeva, V. V. Golovina, M. E. Minyaev, A. V. Lalov, V. M. Pechennikov, V. T. Novikov, M. P. Egorov and M. A. Syroeshkin, *New J. Chem.*, 2023, **47**, 11890–11902.
36 G. N. Schrauzer, R. K. Chadha, C. Zhang and H. K. Reddy, *Chem. Ber.*, 1993, **126**, 2367–2371.
37 M. H. Chisholm, E. E. Delbridge and J. C. Gallucci, *New J. Chem.*, 2004, **28**, 145–152.
38 N. Singh, K. Kumar, N. Srivastav, R. Singh, V. Kaur, J. P. Jasinski and R. J. Butcher, *New J. Chem.*, 2018, **42**, 8756–8764.
39 X. Guo, M. Baumgarten and K. Müllen, *Prog. Polym. Sci.*, 2013, **38**, 1832–1908.
40 A. C. Grimsdale, K. L. Chan, R. E. Martin, P. G. Jokisz and A. B. Holmes, *Chem. Rev.*, 2009, **109**, 897–1091.
41 A. Facchetti, *Chem. Mater.*, 2011, **23**, 733–758.
42 J. Yu, Y. Rong, C.-T. Kuo, X.-H. Zhou and D. T. Chiu, *Anal. Chem.*, 2017, **89**, 42–56.
43 D. T. McQuade, A. E. Pullen and T. M. Swager, *Chem. Rev.*, 2000, **100**, 2537–2574.
44 X. Qian and B. Städler, *Chem. Mater.*, 2019, **31**, 1196–1222.
45 S. Ito, M. Gon, K. Tanaka and Y. Chujo, *Polym. Chem.*, 2021, **12**, 6372–6380.
46 M. Miyata and Y. Chujo, *Polym. J.*, 2002, **34**, 967–969.
47 H. Li and F. Jäkle, *Angew. Chem., Int. Ed.*, 2009, **48**, 2313–2316.
48 A. Sundararaman, M. Victor, R. Varughese and F. Jäkle, *J. Am. Chem. Soc.*, 2005, **127**, 13748–13749.
49 Y. Matsumura, M. Ishidoshiro, Y. Irie, H. Imoto, K. Naka, K. Tanaka, S. Inagi and I. Tomita, *Angew. Chem., Int. Ed.*, 2016, **55**, 15040–15043.
50 Y. Adachi, F. Arai, M. Sakabe and J. Ohshita, *Polym. Chem.*, 2021, **12**, 3471–3477.
51 I. A. Adams and P. A. Rupar, *Macromol. Rapid Commun.*, 2015, **36**, 1336–1340.
52 Y. Chujo and K. Tanaka, *Bull. Chem. Soc. Jpn.*, 2015, **88**, 633–643.
53 M. Gon, K. Tanaka and Y. Chujo, *Polym. J.*, 2018, **50**, 109–126.
54 M. Gon, K. Tanaka and Y. Chujo, *Chem. Rec.*, 2021, **21**, 1358–1373.
55 T. Kato, M. Gon, K. Tanaka and Y. Chujo, *J. Polym. Sci.*, 2021, **59**, 1596–1602.
56 M. Kanjo, M. Gon and K. Tanaka, *ACS Appl. Mater. Interfaces*, 2023, **15**, 31927–31934.
57 S. Ito, M. Fukuyama, K. Tanaka and Y. Chujo, *Macromol. Chem. Phys.*, 2022, **223**, 2100504.
58 K. Suenaga, K. Uemura, K. Tanaka and Y. Chujo, *Polym. Chem.*, 2020, **11**, 1127–1133.
59 R. Yoshii, A. Hirose, K. Tanaka and Y. Chujo, *J. Am. Chem. Soc.*, 2014, **136**, 18131–18139.
60 A. Hirose, K. Tanaka, R. Yoshii and Y. Chujo, *Polym. Chem.*, 2015, **6**, 5590–5595.
61 M. Gon, M. Yaegashi, K. Tanaka and Y. Chujo, *Chem. – Eur. J.*, 2023, **29**, e202203423.
62 M. Gon, M. Yaegashi and K. Tanaka, *Bull. Chem. Soc. Jpn.*, 2023, **96**, 778–784.
63 M. Gon, K. Tanaka and Y. Chujo, *Chem. – Eur. J.*, 2021, **27**, 7561–7571.
64 M. Gon, K. Tanimura, M. Yaegashi, K. Tanaka and Y. Chujo, *Polym. J.*, 2021, **53**, 1241–1249.
65 M. Gon, Y. Morisaki, K. Tanimura, K. Tanaka and Y. Chujo, *Mater. Chem. Front.*, 2023, **7**, 1345–1353.
66 K. Tanimura, M. Gon and K. Tanaka, *Inorg. Chem.*, 2023, **62**, 4590–4597.
67 D. Milstein and J. K. Stille, *J. Am. Chem. Soc.*, 1978, **100**, 3636–3638.
68 M. Kosugi, Y. Shimizu and T. Migita, *J. Organomet. Chem.*, 1977, **129**, C36–C38.
69 J. Otera, T. Hinoishi and H. Okawara, *J. Organomet. Chem.*, 1980, **6**, 93–94.
70 V. M. S. Gil and N. C. Oliveira, *J. Chem. Educ.*, 1990, **67**, 473–478.
71 M. Gon, K. Tanaka and Y. Chujo, *Bull. Chem. Soc. Jpn.*, 2019, **92**, 7–18.
72 E. D. Glendening, C. R. Landis and F. Weinhold, *Wiley Interdiscip. Rev.: Comput. Mol. Sci.*, 2012, **2**, 1–42.
73 A. E. Reed, L. A. Curtiss and F. Weinhold, *Chem. Rev.*, 1988, **88**, 899–926.
74 G. Iasilli, F. Martini, P. Minei, G. Ruggeri and A. Pucci, *Faraday Discuss.*, 2017, **196**, 113–129.
75 I. Platonova, A. Branchi, M. Lessi, G. Ruggeri, F. Bellina and A. Pucci, *Dyes Pigm.*, 2014, **110**, 249–255.
76 S.-L. Li, M. Li, Y. Zhang, H.-M. Xu and X.-M. Zhang, *Inorg. Chem.*, 2020, **59**, 9047–9054.
77 M. Borelli, G. Iasilli, P. Minei and A. Pucci, *Molecules*, 2017, **22**, 1306.